

A. Huber, G. Arnoux, M.N.A. Beurskens, S. Brezinsek, P. Coad, T. Eich, J.C. Fuchs, W. Fundamenski, S. Jachmich, A. Korotkov, A. Loarte, A.G. Meigs, G.F. Matthews, Ph. Mertens, V. Philipps, R.A. Pitts, U. Samm, G. Sergienko, B. Schweer, M.F. Stamp, H. Thomsen and JET EFDA contributors

# Impact of Large Type I ELMs on Plasma Radiation in JET

“This document is intended for publication in the open literature. It is made available on the understanding that it may not be further circulated and extracts or references may not be published prior to publication of the original when applicable, or without the consent of the Publications Officer, EFDA, Culham Science Centre, Abingdon, Oxon, OX14 3DB, UK.”

“Enquiries about Copyright and reproduction should be addressed to the Publications Officer, EFDA, Culham Science Centre, Abingdon, Oxon, OX14 3DB, UK.”

# Impact of Large Type I ELMs on Plasma Radiation in JET

A. Huber<sup>1</sup>, G. Arnoux<sup>2</sup>, M.N.A. Beurskens<sup>2</sup>, S. Brezinsek<sup>1</sup>, P. Coad<sup>2</sup>, T. Eich<sup>3</sup>, J.C. Fuchs<sup>3</sup>,  
W. Fundamenski<sup>2</sup>, S. Jachmich<sup>4</sup>, A. Korotkov<sup>2</sup>, A. Loarte<sup>5</sup>, A.G. Meigs<sup>2</sup>, G.F. Matthews<sup>2</sup>,  
Ph. Mertens<sup>1</sup>, V. Philipps<sup>1</sup>, R.A. Pitts<sup>5</sup>, U. Samm<sup>1</sup>, G. Sergienko<sup>1</sup>, B. Schweer<sup>1</sup>,  
M.F. Stamp<sup>2</sup>, H. Thomsen<sup>3</sup> and JET EFDA contributors\*

*JET-EFDA, Culham Science Centre, OX14 3DB, Abingdon, UK*

<sup>1</sup>*Forschungszentrum Jülich GmbH, Association EURATOM-FZ Jülich, Institut für Plasmaphysik,  
Trilateral Euregio Cluster, D-52425 Jülich, Germany*

<sup>2</sup>*EURATOM-UKAEA Fusion Association, Culham Science Centre, OX14 3DB, Abingdon, OXON, UK*

<sup>3</sup>*Max-Planck-Institut für Plasmaphysik, EURATOM Association, 85748 Garching, Germany*

<sup>4</sup>*Association EURATOM-Belgian State, Koninklijke Militaire School - Ecole Royale Militaire, B-1000 Brussels Belgium*

*\* See annex of F. Romanelli et al, "Overview of JET Results",  
(Proc. 22<sup>nd</sup> IAEA Fusion Energy Conference, Geneva, Switzerland (2008)).*

Preprint of Paper to be submitted for publication in Proceedings of the  
36th EPS Conference on Plasma Physics, Sofia, Bulgaria.  
(29th June 2009 - 3rd July 2009)



## 1. INTRODUCTION

The baseline scenario for ITER operation with high fusion gain ( $Q_{DT} \geq 10$ ) and with high plasma energy ( $\sim 350$  MJ) [1] is the Type I ELMy H-mode regime. The major drawback of this operating regime is the periodic power loading of plasma-facing components by Edge Localised Modes (ELMs) which can cause high target erosion and a significant reduction of component lifetimes. To prevent unacceptable divertor target erosion due to ELMs, the loss in plasma stored energy at the single ELM should be restricted to  $\Delta W_{ELM} \sim 1$  MJ [2] corresponding to the energy density at divertor target of  $0.4$  MJ/m<sup>2</sup>. Only the JET tokamak, thanks to its size, can produce ELMs in the order of 1 MJ with energy densities comparable to the ITER. This contribution focuses on the investigation of the impact of large Type I ELMs on plasma radiation and on power load.

## 2. RESULTS AND DISCUSSION

A series of dedicated discharges with both strike points symmetrically on the lower vertical targets, with identical plasma shape ( $\delta = 0.25$ ,  $\kappa = 1.74$ ), has been performed in the JET Mark II HD divertor configuration with  $I_p = 3$  MA,  $B_T = 3$  T,  $q_{95} = 3.15$ , the stored plasma energy  $W_{plasma} \sim 8$  MJ and a total injected energy of  $\sim 195$  MJ to study the impact of large ELMs on plasma radiation in JET. The gas fuelling is progressively reduced from pulse to pulse, producing Type I ELMs with ELM losses:  $\Delta W_{ELM}$  in the range  $0.25$ – $1.30$  MJ, where  $\Delta W_{ELM}$  is defined as the drop of energy stored within the pedestal on the time scale of several ms as measured by diamagnetic loops. Fig. 1 shows typical time traces of the parameters of an ELMy H-mode discharge in JET with strike points on the vertical tiles – comparable to the standard ITER configuration. The gas fuelling was switched off after 14s, what leads to a transition from a moderate regime of ELMs with  $\Delta W_{ELM} \approx 0.3$ – $0.6$  MJ to the regime with large (giant) ELMs ( $\Delta W_{ELM} \approx 1.3$  MJ). Such ELMs are often followed by a phase of Type III ELMs (so-called “compound” phase) or even a back-transition to Lmode confinement is possible. The “global energy balance” for this discharge (energy balance integrated over the entire discharge) reads: total injected energy of  $E_{in} = 195$  MJ, radiated energy  $E_{rad} = 73$  MJ,  $E_{rad}/E_{in} = 0.47$  and deposited energies onto inner and outer divertor targets of  $24.6$  MJ and  $70.9$  MJ respectively. The largest ELMs deposit on average  $\sim 10\%$  of  $\Delta W_{ELM}$  on the main wall surfaces [3].

Despite the large influence of the gas fuelling on the ELM behaviour, the global energy balance shows negligible variations with different gas levels and correspondingly with different ELM sizes.

A significant part of the total ELM energy loss is in the form of plasma radiation, located mostly in the divertor region. Please note that the radiation is integrated over  $\sim 2$  ms, which is considerably longer than the ELM target power deposition peak of several  $100 \mu$ s. Figure 2 shows the radiation distribution, reconstructed with the aid of the improved\_JET bolometer system [4], for Type I ELMs with medium ( $1\% \leq \Delta W_{ELM}/W \leq 5\%$ ), large ( $5\% \leq \Delta W_{ELM}/W < 9\%$ ) and giant ( $\Delta W_{ELM}/W \geq 9\%$ ) corresponding to ELM energy losses above  $\Delta W_{tr}^{ELM}$  (see the description below) sizes. In all cases, the radiation distribution is strongly weighted to the inner divertor region (in-out asymmetries of  $\sim$  factor 3). The total radiated energies during the Type I ELM normalised to the ELM energy

losses, evaluated by an algorithm similar to that described in [5], are 44%, 53% and 85% for medium, large and giant ELM sizes, respectively. It is important to note that the radiated power is determined by the radiation from the particle release due to the ELM-target interaction together with the changes in the local plasma parameters provoked by the ELM. For ELMs with  $\Delta W_{\text{ELM}} \geq 0.6 \text{ MJ}$  the radiation “spills over” into the outboard X-point region. In the case of the giant ELMs significant radiation is located in the main chamber.

Figure 3 presents the dependence of the radiated plasma energy which follows the ELM crash on the ELM energy drop  $\Delta W_{\text{ELM}}$ . In this case the radiated energy includes only the radiated losses during the first main peak of the ELM. For ELM energy below  $\Delta W_{\text{tr}}^{\text{ELM}} \approx 0.72 \text{ MJ}$ , the radiated plasma energy is proportional to the ELM energy, as expected from the observed linear correlation between impurity influxes and ELM sizes. In this range,  $\sim 50\%$  of the ELM energy drop radiates with the ELM. For a  $\Delta W_{\text{ELM}}$  larger than  $\sim 0.72 \text{ MJ}$ , a non-linear increase of the divertor radiation occurs which is interpreted as an indication of additional carbon ejection from the target tiles made of carbonfibre composites and covered with substantial carbon deposits, possibly due to thermal decomposition and ablation of these layers in the inner divertor. The ELM-induced radiation is always higher at the inner than at the outer divertor with the asymmetry increasing approximately linearly up to a total  $\Delta W_{\text{ELM}}$  of about  $0.6 \text{ MJ}$  and decreasing for higher  $\Delta W_{\text{ELM}}$ . Additionally, Fig 3 shows the radiation fraction in the divertor region as well the Radiated Peaking Factors (RPFs), the local radiation power load onto the wall normalised to the power load averaged over the entire surface, at the Inner Strike Point (ISP). The radiation fraction in the divertor region, defined as ratio of the radiation power below  $Z \leq -1.0 \text{ m}$  (radiated power in the divertor) to the total radiation power, is significant over the entire range of the observed ELM sizes:  $P_{\text{rad}}^{\text{div}}/P_{\text{rad}}^{\text{tot}} \approx 0.8$  for  $\Delta W_{\text{ELM}} < \Delta W_{\text{tr}}^{\text{ELM}}$  and  $P_{\text{rad}}^{\text{div}}/P_{\text{rad}}^{\text{tot}}$  varying between 0.8 to 0.6 for  $\Delta W_{\text{ELM}} > \Delta W_{\text{tr}}^{\text{ELM}}$ . For an ELM energy below  $\Delta W_{\text{tr}}^{\text{ELM}}$ , the radiation peaking factors vary slightly around the averaged value of 2.8. A linear decrease of the RPFs up to value of 1.7 at  $\Delta W_{\text{ELM}} = 1.3 \text{ MJ}$  has been observed above  $\Delta W_{\text{ELM}} > \Delta W_{\text{tr}}^{\text{ELM}}$ . For a giant ELM, shown in the Fig.2, with  $\Delta W_{\text{ELM}} \approx 1.3 \text{ MJ}$  and  $E_{\text{rad}}^{\text{ELM}} 1.1 \text{ MJ}$ , the radiation load on the inner target at the ISP is about  $20 \text{ MW/m}^2$  using the RPF=2 and assuming the radiation heat load time of 2ms. This additional radiation heat load leads to the maximum excursions of  $\sim 100^\circ \text{C}$  at the inner strike point.

Along with the critical question of the radiated energy during the Type I phase (first spike), the radiated energy during the compound phase is an important parameter. The variation of some plasma parameters during the different phases (phase with ELM crashes, compound phase and the recovery phase) of the Type I giant ELM is depicted in Fig.4. The right hand side of the figure shows the stored energy, radiated power and energy. It illustrates the strong degradation of the plasma energy during the compound phase; analysis of the radiation occurring during this phase shows that it accounts for a significant fraction (up to 80% at this ELM) of the plasma energy loss. No significant energy deposition on main wall surfaces in compound phases has been observed [3]. The left hand side of Fig.4 shows the corresponding  $T_e$  and  $n_e$  profiles at the outer mid-plane during the different

phases measured by High Resolution Thomson Scattering (HRTS) system [6]. The collapse of  $T_e$  at the pedestal by 50% follows directly the ELM crash. A reduction of max. 25% of  $n_e$  in the edge region (between 3.6m and 3.75m) has been also observed directly after the ELM crash. The degradation of the confinement during the compound phase is accompanied by a large density reduction right across the plasma profile and loose or reduction of the edge transport barrier associated with density pumpout. On the other hand, the  $T_e$  profile does not show any significant changes during the compound phase. In opposite to the  $T_e$  profile, the  $n_e$  profile needs the entire recovery phase to restore the barrier and the original shape.

The time evolution of different plasma parameters for an ELM with medium and large energy drop is depicted in Fig.5. The figure shows the stored energy, radiated energy,  $D\gamma/D\alpha$  and  $D\beta/D\alpha$  ratios as well as the pedestal parameters. In both cases the surface temperature at inner strike point was significantly over 1000°C, leading, in addition to the impurity influxes associated with transient events, to the deuterium release from the co-deposited carbon layers at the inner strike point. A comparison with results from the laser desorption experiments shows that more than 95% of hydrogen in thin a-C:D layers (<1µm) can be released in a single laser pulse (0.5ms÷3ms duration) [7]. The surface temperature should reach at least 1000°C and we expect the release of the entire D inventory in the layer during a single ELM. The impurity influxes accompanied by the deuterium release can have a significant influence on the discharge since they can lead to a strong divertor cooling, to an increased plasma contamination and even to a radiative collapse. In the case of a large ELM, the  $D\gamma/D\alpha$  and  $(D\beta/D\alpha)$  ratio illustrates an increase by factor of 2.5 (1.8) in the inner divertor region, which is attributed to the onset of recombination and is correlated with detachment [8]. The inner divertor remains detached over the entire compound phase and returns to the attached status in the recovery phase. Short detachment phases have been observed directly after medium size ELMs.

## SUMMARY AND CONCLUSIONS

- Large type I ELMs with losses over 0.72MJ show enhanced radiation losses associated with an ablation of the redeposited carbon layer in the inner divertor.
- Surface (layer) temperatures do not exceed ~ 2000°C at inner target. The surface temperature is too low for bulk carbon ablation but provokes ablation of the deposited layers.
- Large ELMs are often compound (Type I ELM followed by Type III ELMs).
- A significant part (up to 80%) of the plasma energy degradation during the compound phase is exhausted by radiation. The degradation of confinement during the compound phase is accompanied by a collapse in pedestal density.
- The “compound” phase indicates an increased plasma contamination, which otherwise does not lead to a radiative collapse of the plasma.
- ELM-induced radiation is always higher at the inner than at the outer divertor: approximately a linear increase in asymmetry up to  $\Delta W_{ELM} \sim 0.6MJ$  then a decrease for higher  $\Delta W_{ELM}$ .
- During the ELMs, the radiation is mostly located in the divertor region.

- Giant ELMs drive the divertor into detachment after the ELM crash. Divertor detachment remains during the entire compound phase.
- Larger ELMs deposit more energy on limiters. No energy is deposited in compound phases.

## ACKNOWLEDGEMENTS

This work, supported by the European Communities under the contract of Association between EURATOM and FZJ, was carried out within the framework of the European Fusion Development Agreement. The views and opinions expressed herein do not necessarily reflect those of the European Commission.

## REFERENCES

- [1]. ITER Physics Basis Editors, Nuclear Fusion **39** (1999) 2137
- [2]. A. Loarte *et al.*, “Power and particle fluxes at the plasma edge of ITER: Specifications and Physics Basis”, 22nd IAEA Fusion Energy Conference, Geneva, Switzerland (2008).
- [3]. R.A. Pitts *et al.*, Journal of Nuclear Materials **390-391** (2009) 755
- [4]. A. Huber, K. McCormick, P. Andrew, *et al.*, Fusion Engineering and Design **82** (2007) 1327.
- [5]. J.C. Fuchs, T. Eich, A. Hermann *et al.*, Journal of Nuclear Materials **337-339** (2005) 756
- [6]. R. Pasqualotto *et al.*, Review Scientific Instruments **75** (2004) 3891
- [7]. B. Schweer *et al.*, Journal of Nuclear Materials **390-391** (2009) 576
- [8]. G.M. McCracken, M.F. Stamp, R.D. Monk *et al.*, Nuclear Fusion **38** (1998) 619

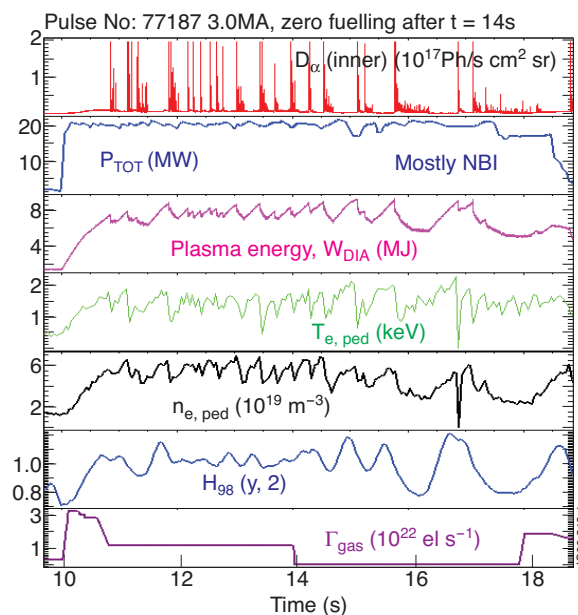


Figure 1: Selected plasma signals for a 3MA H-mode discharge.



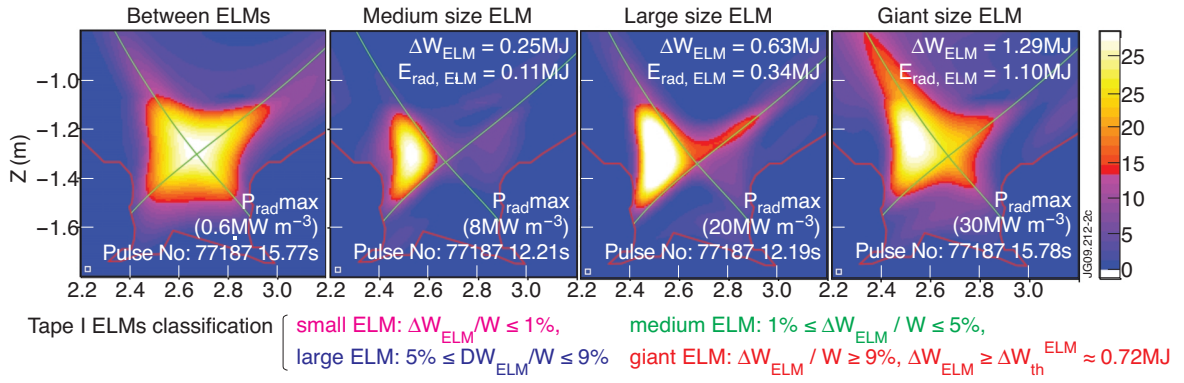


Figure 2: Radiation distribution between ELMs, radiation distributions integrated over the ELM crashes during the middle size and large size ELMs as well as during the giant ELM.

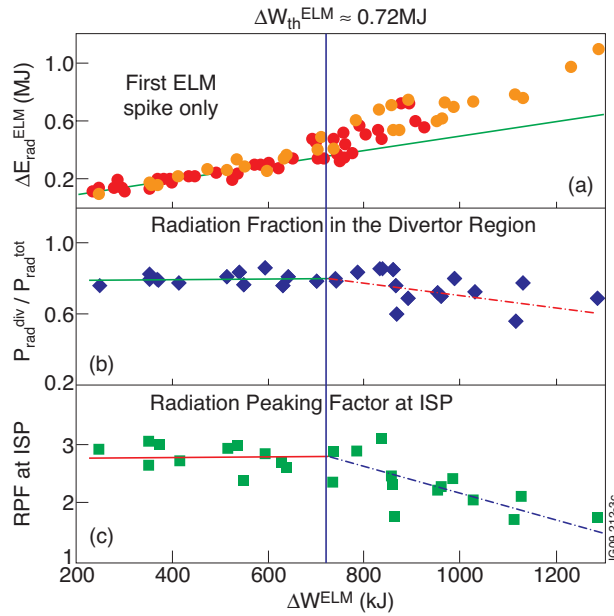


Figure 3: Radiated plasma energy (a), divertor radiation fraction (b) and radiated peaking factor (c) at the inner strike point (ISP).

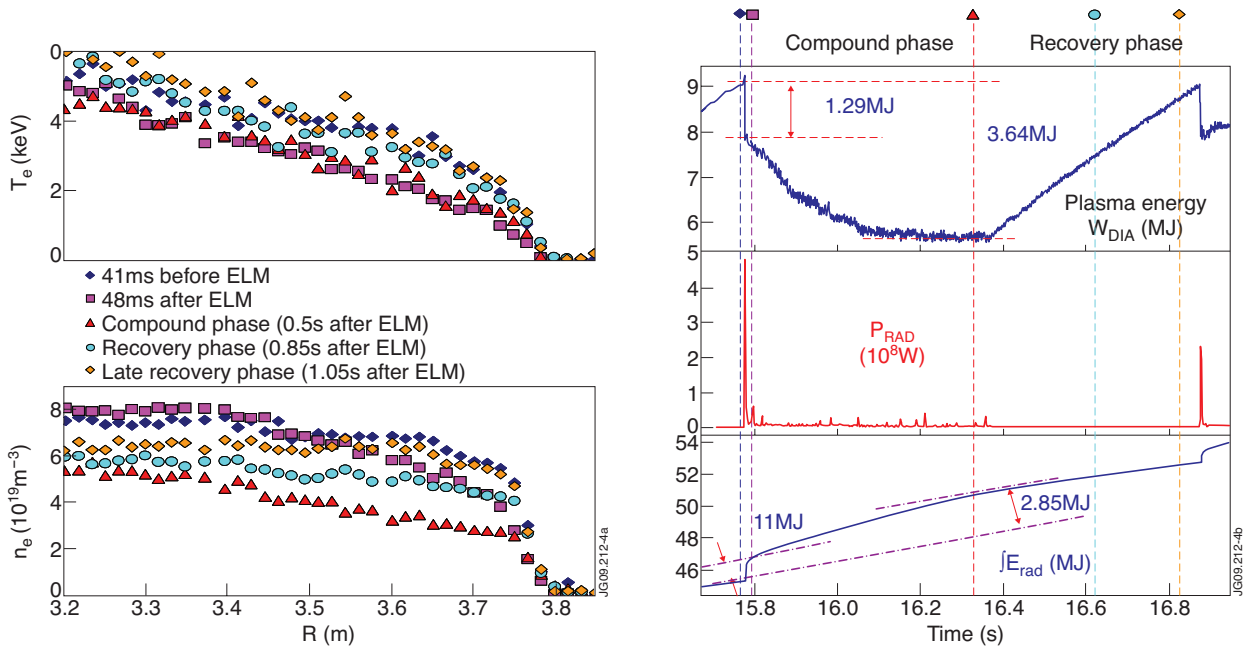


Figure 4: Plasma behaviour during the different phases of Type I giant ELM.

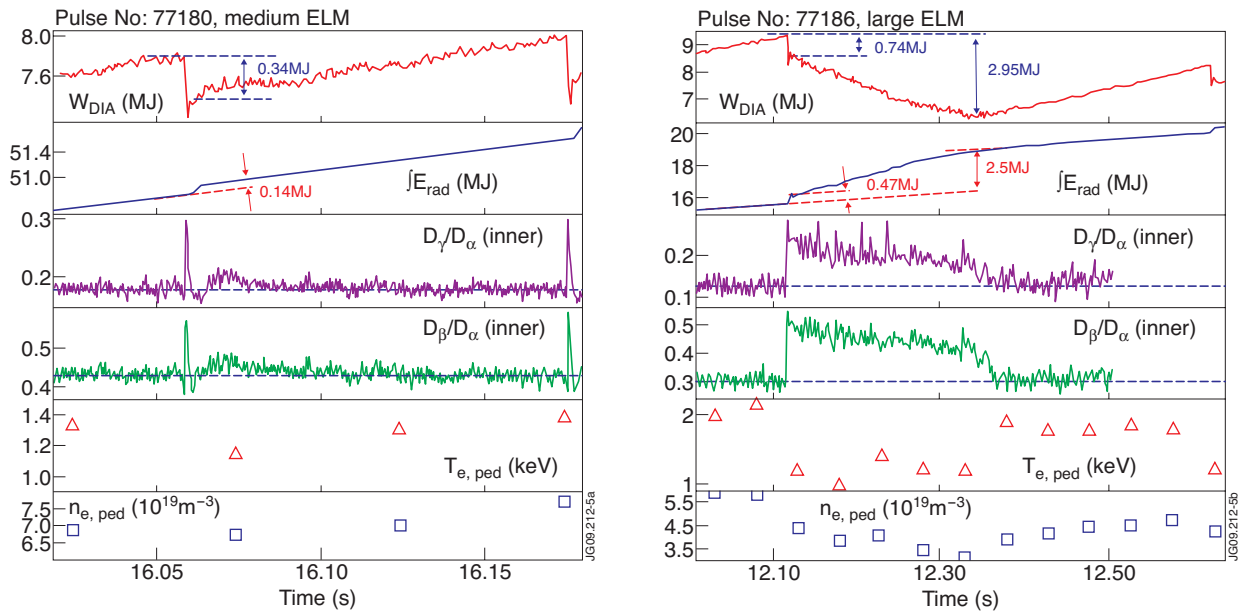


Figure 5: Comparison of ELM with medium and large sizes.